American Mineralogist, Volume 91, pages 1909–1917, 2006

Phosphohedyphane, $Ca_2Pb_3(PO_4)_3Cl$, the phosphate analog of hedyphane: Description and crystal structure

ANTHONY R. KAMPF,[1,*] IAN M. STEELE,[2] AND ROBERT A. JENKINS[3]

[1]Mineral Sciences Department, Natural History Museum of Los Angeles County, 900 Exposition Boulevard, Los Angeles, California 90007, U.S.A.
[2]Department of the Geophysical Sciences, The University of Chicago, 5734 South Ellis Avenue, Chicago, Illinois 60637, U.S.A.
[3]4521 North Via Madre, Tucson, Arizona 85749, U.S.A.

ABSTRACT

Phosphohedyphane, $Ca_2Pb_3(PO_4)_3Cl$, space group $P6_3/m$, $a = 9.857(1)$, $c = 7.130(2)$ Å, $V = 599.9(2)$ Å^3, $Z = 2$, is a new mineral from the Capitana mine, Copiapó, Atacama Province, Chile and has been identified from numerous other deposits world-wide. At the Capitana mine, it occurs as transparent, colorless, tapering hexagonal prisms, as individuals up to about 0.5 mm in length and 0.1 mm in diameter, which are commonly doubly terminated. Crystals often occur in subparallel intergrowths and irregular clusters. Phosphohedyphane forms as a secondary mineral in the oxidized zone of the Capitana mine, a Cu-Pb-Ag deposit, where it closely associated with quartz, duftite, and bayldonite. Crystals exhibit core-to-rim chemical zonation and electron analyses of cores/rims yielded CaO 9.24/7.76, PbO 67.60/69.35, P_2O_5 18.40/17.00, As_2O_5 2.73/3.68, Cl 3.32/3.22, –O = Cl –0.75/–0.73, total 100.54/100.28 wt%. The name phosphohedyphane is for the relationship of the mineral to hedyphane. The mineral has an apatite structure with ordering of Ca and Pb in the two non-equivalent large cation sites, as in hedyphane. The structure refinement indicates that the Ca2(6*h*) site is completely occupied by Pb and the Ca1(4*f*) site is occupied by 92% Ca and 8% Pb. The tetrahedral site refines to 91% P and 9% As. The refinement indicates the 0,0,0 position to be fully occupied by Cl. The ordering of Ca and Pb in phosphohedyphane has important implications with respect to the chlorapatite-pyromorphite solid solution series. An analysis of compositions of natural members of the pyromorphite-mimetite-turneaureite-chlorapatite system suggests the existence of complete solid solution among pyromorphite, mimetite, hedyphane, and phosphohedyphane. No stable solid solutions appear to exist between the joins phosphohedyphane-hedyphane and chlorapatite-turneaureite in natural systems.

Keywords: Phosphohedyphane, new mineral, crystal structure, chemical analysis, solid solution, pyromorphite, apatite group

INTRODUCTION

Dating back to the discovery of the famous "Chañarcillo" silver deposit in 1832 (Cook 1979), the mines around Copiapó in the Atacama Desert of Chile have been yielding a remarkable array of unusual minerals. In 2004 at the Capitana mine near Copiapó, one of the authors (R.A.J.) collected specimens containing crystals of the new mineral species reported herein.

The new species with ideal formula $Ca_2Pb_3(PO_4)_3Cl$ is a phosphate member of the apatite group with Ca and Pb ordered in the two cation sites. The strong preference of Pb^{2+} for the Ca2(6*h*) site in the apatite structure has been previously shown by single-crystal and powder XRD studies of synthetic Pb-bearing apatites (Engel et al. 1975; Hata et al. 1980; Mathew et al. 1980; Verbeeck et al. 1981). Similar ordering occurs in the mineral caracolite, $Na_3Pb_2(SO_4)_3Cl$, (Schneider 1967) and the same ordering in hedyphane, $Ca_2Pb_3(AsO_4)_3Cl$ (Rouse et al. 1984). The new mineral can be regarded as the phosphate analog of hedyphane and, for this reason, has been named phosphohedyphane.

The new mineral and name have been approved by the Commission on New Minerals and Mineral Names of the International Mineralogical Association. The holotype specimen is housed in the mineral collection of the Natural History Museum of Los Angeles County (catalog number 55429).

OCCURRENCE

The new mineral occurs on specimens collected from the dumps of the southern workings of the Capitana mine. Three samples were found on different parts of the dumps, but to date none have been encountered in the accessible underground or open pit parts of the mine. There is no question that the samples came from the mine, as the matrix and alteration found in the phosphohedyphane samples closely match most of the oxidization-zone rocks from the mine. The mineral is closely associated with quartz, duftite, and bayldonite. Other secondary minerals identified in the oxidized zone include anglesite, arsentsumebite, azurite, beaverite, calcite, cerussite, mimetite, malachite, mottramite, and perroudite.

The Capitana mine is located 18.6 km due east of the central plaza in Copiapó at a division of Quebrada Cinchado (Cinchado arroyo or dry wash). The mineralization is found in conglomerates of the Checo de Cobre member of the Cerillos formation of lower Cretaceous age (Segerstrom 1960). The mine has two, 1 to 2 meter wide vertical quartz-barite veins that were mined

* E-mail: akampf@nhm.org

for copper, lead, and silver: one vein strikes N50°E and the other N80°W (Segerstrom 1960; Bruggen 1938). Vanadium was also reported from the Capitana mine as a copper-lead vanadate (probably mottramite) (Risopatron 1928) and as a vanadium silicate (Bruggen 1938).

The occurrence of phosphohedyphane has also been confirmed, both by powder XRD and electron microprobe investigations, in oxidized zone mineralization at the Root mine (Goodsprings district, Clark Co., Nevada) and the Silver Coin mine (Iron Point district, Humboldt Co., Nevada). Similarly, samples previously identified as pyromorphite from numerous localities around the world, were surveyed by semi-quantitative EDS analyses (Table 1). The results indicate that phosphohedyphane also occurs at the Argentena, Mobile, and Monte Cristo mines (Goodsprings district, Nevada), the Great Eastern mine (Cochise Co., Arizona), the Hardshell mine (Patagonia Mts., Arizona), the Mammoth mine (Tiger, Arizona), the Tonopah-Belmont mine (Tonopah, Arizona), the Broken Hill mine (New South Wales, Australia), Tennant Creek (Northern Territory, Australia), Laurium (Attica, Greece), and the Berezovskoye mines (Urals, Russia). Reinvestigation of chemical analyses of Ca-bearing pyromorphites provided by Dana (1892) yield similar conclusions. These analyses indicate that material from the Sonnenwirbel mine, Freiberg, Saxony, Germany (named polysphaerite by Breithaupt 1832) and from Nuizière, Rhône, France (named nussièrite by Barruel 1836) are probably phosphohedyphane. A new microprobe analysis (N.V. Chukanov and I.V. Pekov, personal communication; Table 2) of thin grayish and white crusts with green pyromorphite reported as "polysphaerite" from oxidized ores of the Ken'-Choku polymetallic deposit in Central Kazakhstan by Chukhrov (1952), are consistent with phosphohedyphane. A recent report by Raade (2005) of clear, colorless, zoned, Ca-rich pyromorphite crystals

TABLE 1. Results of EDS survey, plus analyses from Table 2 and selected analyses from Rouse et al. (1984), Dana (1892), and Palache et al. (1951)

Location	Description	Species†	Ca‡	P§
Brown's pros., Rum Jungle, No. Terr., Australia	deep green bundles of prisms	pyromorphite	0.0	0.95
Tennant Creek, Northern Territory, Australia	green-yellow tapering crystals	phosphohedyphane	1.4	1.00
Broken Hill, New South Wales, Australia	clear colorless prisms	phosphohedyphane	1.3	0.95
Broken Hill, New South Wales, Australia	white stout prisms	pyromorphite	0.4	1.00
Broken Hill, New South Wales, Australia	clear brown prisms	pyromorphite	0.0	1.00
Broken Hill, New South Wales, Australia	green-yellow tapering prisms	pyromorphite	0.0	1.00
Broken Hill, New South Wales, Australia	yellow tablets	pyromorphite	0.0	0.95
Broken Hill, New South Wales, Australia	deep yellow stout prisms	mimetite	0.0	0.10
Mount Isa, Queensland, Australia	pale yellow stout prisms	pyromorphite	0.3	1.00
Platt mine, Dundas, Tasmania, Australia	clear dark green prisms	pyromorphite	0.0	1.00
Sylvester mine, Zeehan, Tasmania, Australia	deep green tapering prisms	pyromorphite	0.0	1.00
Longvilly, Luxembourg, Belgium	yellow-green prisms	pyromorphite	0.0	1.00
Llallagua, Potosi dept., Bolivia	gray-green rounded prisms	pyromorphite	0.0	1.00
Society Girl mine, Moyie, BC, Canada	green-yellow barrel-shaped prisms	pyromorphite	0.1	1.00
Capitana mine, Copiapo, Atacama, Chile	colorless tapering prisms (cores)*	phosphohedyphane	1.8	0.90
Capitana mine, Copiapo, Atacama, Chile	colorless tapering prisms (rims)*	phosphohedyphane	1.5	0.90
Grande mine, Arqueros, Coquimbo, Chile	(Palache et al. 1951)	hedyphane	1.6	0.40
Daoping mine, Guilin, Guangxi, China	yellow-green prisms	pyromorphite	0.1	1.00
Stříbro, Bohemia, Czech Republic	pale yellow prisms	pyromorphite	0.4	0.90
Stříbro, Bohemia, Czech Republic	brown (Dana 1892)	calcian pyromorphite	0.8	1.00
Villevielle, Pontigibaud, Auvergne, France	(Palache et al. 1951)	calcian mimetite	0.8	0.20
Ussel, Corrèze, France	cream-colored xls	pyromorphite	0.2	1.00
Les Farges mine, Ussel, Corrèze, France	deep green prisms	pyromorphite	0.0	1.00
Les Farges mine, Ussel, Corrèze, France	yellow prisms	pyromorphite	0.0	0.70
Nuizière, Rhône, France	greenish yellow (Dana 1892)	phosphohedyphane	2.4	0.90
Badenweiler, Baden-Württemberg, Germany	way-yellow (Dana 1892)	calcian pyromorphite	0.5	1.00
Schapbach, Baden-Württemberg, Germany	green (Dana 1892)	calcian pyromorphite	0.7	1.00
Schauinsland dist., Baden-Württemberg, Germany	yellow-green prisms	pyromorphite	0.3	1.00
Krandorf, Bavaria, Germany	green prisms	pyromorphite	0.1	1.00
Bad Ems dist., Rheinland-Palatinate, Germany	pale gray prisms	pyromorphite	0.3	1.00
Bad Ems dist., Rheinland-Palatinate, Germany	colorless composite prisms	pyromorphite	0.2	1.00
Braubach, Bad Ems dist., Rh.-Pal., Germany	pale gray prisms	pyromorphite	0.3	1.00
Friedrichssegen mine, Bad Ems dist., Rh.-Pal., Ger.	yellow-green prisms	pyromorphite	0.1	0.85
Sonnenwirbel mine, Freiberg, Saxony, Germany	(Dana 1892)	phosphohedyphane	1.3	1.00
Friedrichroda, Thuringia, Germany	green prisms	pyromorphite	0.0	1.00
Laurium, Attica, Greece	gray-green steep pyramids	phosphohedyphane	1.6	0.85
Arbus, Sardinia, Italy	colorless acicular	pyromorphite	0.0	1.00
Montevecchio, Sardinia, Italy	pale green bundles of prisms	calcian pyromorphite	0.8	1.00
Ogoya mine, Ishikawa Pref., Japan	lime-green prisms	pyromorphite	0.0	1.00
Ken'-Choku, Central Kazakhstan	light-gray curved prisms*	phosphohedyphane	1.9	1.00
San Antonio mine, Santa Eulalia, Chi., Mexico	light yellow tapering prisms	mimetite	0.0	0.00
Potosi mine, Santa Eulalia, Chihuahua, Mexico	light green-yellow prisms	pyromorphite	0.0	1.00
Ojuela mine, Mapimi, Durango, Mexico	colorless bundles of prisms	hedyphane	1.0	0.00
Ojuela mine, Mapimi, Durango, Mexico	yellow prisms	mimetite	0.0	0.00
Ojuela mine, Mapimi, Durango, Mexico	light yellow-green prisms	pyromorphite	0.0	1.00
Tsumeb, Namibia	(Palache et al. 1951)	calcian mimetite	0.7	0.10

Notes: A variety of other cations occurring in small amounts are not reported and have not been factored into the above cation ratios.
* Marked samples represent analyses from Table 2.
† The calcian modifier is used here for pyromorphite or mimetite with Ca ≥ 0.5 per formula unit (CaO > 2%).
‡ Ca atoms in formula unit [5 ×Ca/(Ca + Pb); to nearest 0.1]; 0 = pyromorphite-mimetite, 2 = phosphohedyphane-hedyphane, 5 = chlorapatite-turneaureite.
§ P atoms relative to total P + As [P/(P + As); to nearest 0.05]; 0 = mimetite-hedyphane-turneaureite, 1 = pyromorphite-phosphohedyphane-chlorapatite.

from Berg Aukas, Grootfontein, Namibia, includes chemical analyses consistent with these crystals being phosphohedyphane. On the other hand, material from Mies (now Stříbro), Bohemia, Czech Republic (Dana 1892; named miesite by Breithaupt 1841), which is close to phosphohedyphane in composition, corresponds to calcian pyromorphite.

TABLE 1.—*Continued*

Location	Description	Species†	Ca‡	P§
Berezovskoye mines, Urals, Russia	cream-colored prisms	phosphohedyphane	1.9	1.00
Argent mine, Gauteng, South Africa	bright yellow-green steep pyramids	pyromorphite	0.0	0.95
Doornhoek mine, Transvaal, South Africa	yellow rounded prisms	pyromorphite	0.1	1.00
Edendale mine, Transvaal, South Africa	yellow-green barrel-shaped prisms	pyromorphite	0.4	1.00
Horcajo mines, Ciudad Real, Spain	colorless prisms	pyromorphite	0.0	1.00
Santa Eufemia, Cordoba, Spain	pale green-yellow prisms	pyromorphite	0.0	1.00
Långban, Varmland, Sweden	134981 (Rouse et al. 1984)	turneaureite	5.0	0.20
Långban, Varmland, Sweden	B13171 (Rouse et al. 1984)	turneaureite	5.0	0.05
Långban, Varmland, Sweden	H105545 (Rouse et al. 1984)	hedyphane	2.3	0.00
Långban, Varmland, Sweden	H90417 (Rouse et al. 1984)	hedyphane	2.1	0.00
Långban, Varmland, Sweden	H101553 (Rouse et al. 1984)	hedyphane	1.5	0.00
Långban, Varmland, Sweden	PA13951 (Rouse et al. 1984)	hedyphane	1.3	0.00
Långban, Varmland, Sweden	H116366 (Rouse et al. 1984)	hedyphane	1.2	0.05
Långban, Varmland, Sweden	green barrel-shaped prisms	calcian pyromorphite	0.6	1.00
Penberthy Croft mine, Cornwall, England, U.K.	clear colorless prisms	mimetite	0.0	0.00
Trevinnick mine, Cornwall, England, U.K.	light green barrel-shaped prisms	pyromorphite	0.2	1.00
Wheal Alfred, Cornwall, England, U.K.	green-yellow prisms	mimetite	0.0	0.45
Dry Gill, Caldbeck Fells, England, U.K.	deep green tapering prisms	calcian pyromorphite	0.7	1.00
Roughton Gill, Caldbeck Fells, England, U.K.	pale yellow thin tapering prisms	pyromorphite	0.0	1.00
Burgam mine, Shropshire, England, U.K.	yellow-green bundles of prisms	pyromorphite	0.0	1.00
Leadhills, Scotland, U.K.	yellow-green prisms	pyromorphite	0.0	1.00
New Glencrief mine, Wanlockhead, Scotland, U.K.	yellow-green xls	pyromorphite	0.4	1.00
Plynlimon Mine, Ceredigon, Wales, U.K.	yellow-green thin tapering prisms	pyromorphite	0.0	1.00
Great Eastern mine, Cochise Co., AZ, U.S.A.	colorless steep pyramids	phosphohedyphane	1.6	1.00
Hardshell mine, Patagonia Mts., AZ, U.S.A.	clear yellow stout prisms	phosphohedyphane	1.2	0.90
Mammoth mine, Tiger, AZ, U.S.A.	yellow acicular	phosphohedyphane	1.6	0.75
Tonopah-Belmont mine, Tonopah, AZ, U.S.A.	colorless tapering prisms	phosphohedyphane	1.3	1.00
Tonopah-Belmont mine, Tonopah, AZ, U.S.A.	colorless tapering prisms	phosphohedyphane	1.2	1.00
Midnight mine, Burke, ID, U.S.A.	cream-colored prisms	pyromorphite	0.0	1.00
Bunker Hill mine, Kellogg, ID, U.S.A.	orange-yellow prisms	pyromorphite	0.0	0.80
Manhan mines, Easthampton, MA, U.S.A.	yellow-green prisms	pyromorphite	0.3	1.00
Butte, Silver Bow Co., MT, U.S.A.	pale green tapering prisms	pyromorphite	0.2	1.00
Thomaston, Litchfield Co., CT, U.S.A.	yellow-green tapering prisms	pyromorphite	0.0	0.90
Argentena mine, Goodsprings dist., NV, U.S.A.	yellow fibers	phosphohedyphane	1.7	0.75
Argentena mine, Goodsprings dist., NV, U.S.A.	yellow composite prisms	phosphohedyphane	1.6	0.70
Argentena mine, Goodsprings dist., NV, U.S.A.	yel.-brown barrel-shaped prisms	phosphohedyphane	1.5	0.75
Argentena mine, Goodsprings dist., NV, U.S.A.	pale yellow fibers	phosphohedyphane	1.3	0.55
Argentena mine, Goodsprings dist., NV, U.S.A.	yellow druse	mimetite	0.2	0.20
Lookout mine, Goodsprings dist., NV, U.S.A.	orange-yellow cauliflower masses	calcian mimetite	0.9	0.45
Mobile mine, Goodsprings dist., NV, U.S.A.	pale yellow-green tapering prisms	phosphohedyphane	1.4	0.80
Monte Cristo mine, Goodsprings dist., NV, U.S.A.	pale yellow crude prisms	phosphohedyphane	1.5	0.70
Monte Cristo mine, Goodsprings dist., NV, U.S.A.	orange-yel. crude prisms	calcian mimetite	0.6	0.40
Monte Cristo mine, Goodsprings dist., NV, U.S.A.	yellow druse	calcian mimetite	0.6	0.35
Mtn. Top mine, Goodsprings dist., NV, U.S.A.	light yellow prisms	mimetite	0.1	0.05
Root mine, Goodsprings dist., NV, U.S.A.	colorless acicular*	phosphohedyphane	1.6	1.00
Root mine, Goodsprings dist., NV, U.S.A.	colorless tapering prisms	phosphohedyphane	1.6	0.70
Root mine, Goodsprings dist., NV, U.S.A.	gray green tapering prisms	phosphohedyphane	1.1	0.80
Root mine, Goodsprings dist., NV, U.S.A.	yellow acicular	phosphohedyphane	1.0	0.60
Singer mine, Goodsprings dist., NV, U.S.A.	colorless bipyramids	hedyphane	1.3	0.30
Singer mine, Goodsprings dist., NV, U.S.A.	lt. yellow clusters of stout prisms*	hedyphane	1.1	0.15
Singer mine, Goodsprings dist., NV, U.S.A.	orange stout prisms	mimetite	0.2	0.00
Singer mine, Goodsprings dist., NV, U.S.A.	orange needles	mimetite	0.1	0.00
Whale mine, Goodsprings dist., NV, U.S.A.	pale green prisms	mimetite	0.4	0.30
Silver Coin mine, Iron Point dist., NV, U.S.A.	colorless thin prisms (cores)*	phosphohedyphane	1.6	0.95
Silver Coin mine, Iron Point dist., NV, U.S.A.	colorless thin prisms (rims)*	calcian pyromorphite	0.5	0.84
San Rafael mine, Lodi dist., NV, U.S.A.	pale green-yellow prisms	mimetite	0.1	0.25
Franklin, Sussex Co., NJ, U.S.A.	C6270-1 (Rouse et al. 1984)	turneaureite	5.0	0.25
Franklin, Sussex Co., NJ, U.S.A.	C6277-1 (Rouse et al. 1984)	hedyphane	2.2	0.00
Franklin, Sussex Co., NJ, U.S.A.	R6552 (Rouse et al. 1984)	hedyphane	1.8	0.05
Franklin, Sussex Co., NJ, U.S.A.	H105459 (Rouse et al. 1984)	hedyphane	1.5	0.05
Franklin, Sussex Co., NJ, U.S.A.	H105462 (Rouse et al. 1984)	hedyphane	1.4	0.10
Silver Hill, Davidson Co., NC, U.S.A.	pink prisms	aluminian pyromorphite	0.0	1.00
Wheatley mines, Phoenixville dist., PA, U.S.A.	yellow-green composite prisms	pyromorphite	0.3	1.00
Cardiff mine, Big Cottonwood dist., UT, U.S.A.	light blue-green composite prisms	pyromorphite	0.0	1.00
Kabwe (Broken Hill) mine, Central Prov., Zambia	colorless crystals	calcian pyromorphite	0.7	1.00
Penhalonga, Manicaland, Zimbabwe	green prisms	pyromorphite	0.0	0.90

Notes: A variety of other cations occurring in small amounts are not reported and have not been factored into the above cation ratios.

* Marked samples represent analyses from Table 2.

† The calcian modifier is used here for pyromorphite or mimetite with Ca ≥ 0.5 per formula unit (CaO > 2%).

‡ Ca atoms in formula unit [5 ×Ca/(Ca + Pb); to nearest 0.1]; 0 = pyromorphite-mimetite, 2 = phosphohedyphane-hedyphane, 5 = chlorapatite-turneaureite.

§ P atoms relative to total P + As [P/(P + As); to nearest 0.05]; 0 = mimetite-hedyphane-turneaureite, 1 = pyromorphite-phosphohedyphane-chlorapatite.

TABLE 2. Electron microprobe analyses in wt%

	CaO	PbO	P_2O_5	As_2O_5	Cl	O=Cl	Total	Empirical Formula*
Phosphohedyphane	10.97	65.51	20.83	0.00	3.47	–0.78	100.00	$Ca_2Pb_3(PO_4)_3Cl$
Capitana mine (cores)†	9.24	67.60	18.40	2.73	3.32	–0.75	100.54	$(Ca_{1.75}Pb_{0.22})Pb_3(P_{0.92}As_{0.08}O_4)_3Cl_{1.00}$
Capitana mine (rims)†	7.76	69.35	17.00	3.68	3.22	–0.73	100.28	$(Ca_{1.53}Pb_{0.44})Pb_3(P_{0.89}As_{0.12}O_4)_3Cl_{1.01}$
Silver Coin mine (cores)†	2.25	78.55	13.70	4.26	2.83	–0.64	100.95	$(Ca_{0.52}Pb_{1.55})Pb_3(P_{0.83}As_{0.16}O_4)_3Cl_{1.03}$
Silver Coin mine (rims)†	8.66	70.02	19.45	1.29	3.33	–0.75	102.00	$(Ca_{1.63}Pb_{0.33})Pb_3(P_{0.97}As_{0.04}O_4)_3Cl_{0.99}$
Root mine†	8.31	70.90	19.20	0.48	3.29	–0.74	101.44	$(Ca_{1.61}Pb_{0.45})Pb_3(P_{0.98}As_{0.02}O_4)_3Cl_{1.01}$
Singer mine†	4.98	68.70	2.27	22.40	2.85	–0.64	100.56	$(Ca_{1.15}Pb_{1.00})Pb_3(P_{0.14}As_{0.84}O_4)_3Cl_{1.04}$
Ken'-Choku, Kazakhstan‡	10.13	66.77	19.48	0.24	2.66	–0.60	99.01	$(Ca_{1.89}Pb_{0.14})Pb_3(P_{0.96}As_{0.01}Si_{0.02}O_4)_3Cl_{0.79}$

* Based on O = 12 apfu.
† Standards: synthetic $Ca_2P_2O_7$ (Ca and P), synthetic PbS (Pb), synthetic $FeAs_2$ (As), synthetic chlorapatite (Cl).
‡ Unpublished data of N.V. Chunkanov and I.V. Pekov (plus 0.33 SiO_2).

PHYSICAL AND OPTICAL PROPERTIES

At the Capitana mine phosphohedyphane forms tapering hexagonal prisms (Fig. 1) up to about 0.5 mm in length and 0.1 mm in diameter, which are commonly doubly terminated. Forms observed are {100} and {101} (good), {411} (poor), and {10.0.1} and {20.0.1} (approx.). Crystals often occur in subparallel intergrowths and irregular clusters and sometimes appear curved, presumably due to growth offsets. Crystal faces sometimes exhibit fine-scale irregular, rounded latitudinal striations or growth markings.

Capitana phosphohedyphane crystals are transparent and colorless, while those from other localities occur in a variety of colors (see Table 1); however, those highest in Ca content tend to be colorless or very pale in color. Crystals exhibit vitreous to greasy luster and have white streak. The mineral is non-fluorescent and has a Mohs hardness of approximately 4. Crystals are brittle, exhibit no cleavage and have subconchoidal fracture. The mineral decomposes quickly in dilute HCl and the residue dissolves slowly. The calculated density based on the composition of crystal cores is 5.92 g/cm^3. Crystals are optically uniaxial (–) with optical constants measured in sodium light (589 nm): ω = 1.935(2) and ε = 1.928(2).

CHEMISTRY

Quantitative chemical analyses of phosphohedyphane were performed by electron microprobe (WDS mode, 15 kV, 25 nA, 5 μm beam diameter). Most crystals on the type specimen are zoned. The crystal cores appear to be reasonably uniform both from the chemical and crystallographic point of view, while the rims, which can account for a significant volume of the crystal, exhibit fine-scale chemical zonation with a radial pattern extending from the core to the outer surface. The rims are evident both from backscatter electron images and under optical examination in immersion liquids. The results of analyses of the cores (two analyses) and rims (four analyses) of two crystals are reported in Table 2 together with analyses for crystals from the Root mine (phosphohedyphane), the Silver Coin mine (zoned phosphohedyphane/calcian pyromorphite), the Singer mine (intermediate mimetite-hedyphane), and Ken'-Choku, Kazakhstan (phosphohedyphane).

The crystal from the Capitana mine used for the structure data collection does not appear to be rimmed and seems to correspond most closely to the chemistry of the cores.

The empirical formula of the cores of phosphohedyphane crystals from the Capitana mine $(Ca_{1.75}Pb_{0.22})Pb_3(P_{0.92}As_{0.08}O_4)_3Cl_{1.00}$ (based on O = 12 apfu) compares favorably with the formula based on the structure analysis $(Ca_{1.84}Pb_{0.16})Pb_3(P_{0.91}As_{0.09}O_4)_3Cl$. The simplified formula is $Ca_2Pb_3(PO_4)_3Cl$, which requires: CaO = 10.97, PbO = 65.51, P_2O_5 = 20.83, Cl = 3.47, –O = Cl = 0.78, total 100.00 wt%. The Gladstone-Dale compatibility index $[1 - (K_P/K_C)]$ is –0.012 (superior), based on the empirical formula, measured indices of refraction and calculated density for the crystal cores.

The semi-quantitative survey of 86 samples previously identified as pyromorphite from numerous localities around the world was performed on a Hitachi S-3000N SEM using an Oxford SEMEDX200. Spectra were obtained from unpolished crystal surfaces, in most cases crystal faces, and thus analyses represent only the outermost portions of crystals. The results of the survey, in terms of the ratios Ca/(Ca + Pb) and P/(P + As), are provided in Table 1, along with the results of the microprobe analyses in Table 2 and those reported for hedyphane and turneaureite by Rouse et al. (1984).

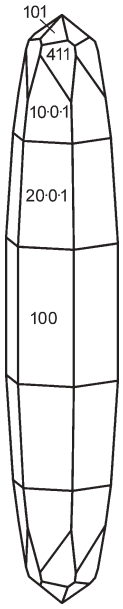

FIGURE 1. Crystal drawing of phosphohedyphane.

X-RAY CRYSTALLOGRAPHY AND STRUCTURE REFINEMENT

X-ray powder-diffraction data (Table 3) were obtained using a Gandolfi camera (114.6 mm diameter, Ni-filtered Cu$K\alpha$ radiation). The data show good agreement with the pattern calculated from the structure. The unit-cell data refined from the 3-circle diffractometer data are provided in Table 4. The powder pattern of phosphohedyphane is easily distinguished from that of pyromorphite (see Table 3); besides relatively small shifts in d-spacing, there are significant intensity differences: phosphohedyphane exhibits much stronger 100, 002, and 122/211 lines and much weaker 200, 102, 120/210, 112, 300, 222, and 140/410 lines. Powder XRD patterns obtained for several other phosphohedyphane and calcian pyromorphite samples from the

EDS survey were all very similar to the aforementioned phosphohedyphane pattern.

Structure data collection was performed on a Bruker PLATFORM 3-circle goniometer equipped with a 1K SMART CCD detector. A hemisphere of three-dimensional data were collected from a tapering prism from the type specimen. Fifty duplicate frames, acquired at the end of the data collection, indicated that no significant decay had taken place. The measured intensities were corrected for Lorentz and polarization effects using the program SAINT and an empirical absorption correction was applied using the program SADABS (Bruker 1997).

The SHELXL97 software (Sheldrick 1997) was used for the refinement of the structure. The R1 (conventional *R* factor) converged to 2.54% for 481 reflections with $F_o > 4\sigma(F_o)$. Table 4 gives the details of the data collection and structure refinement; Table 5, the final fractional coordinates and isotropic displacement parameters; Table 6, the anisotropic displacement parameters; Table 7, interatomic distances compared to those in hedyphane; and Table 8, bond valences.

TABLE 3. Observed and calculated X-ray powder-diffraction pattern for phosphohedyphane compared to calculated pattern for pyromorphite

Phosphohedyphane				Pyromorphite		
I_{obs}	d_{obs}	d_{calc}	I_{calc}	I_{calc}	d_{calc}	*hkl*
20	8.538	8.536	18	1	8.640	100
5	4.937	4.928	9	10	4.988	110
5	4.266	4.268	7	29	4.320	200
60	4.054	4.054	50	45	4.128	111
30	3.565	3.565	26	7	3.676	002
5	3.287	3.290	8	30	3.382	102
10	3.223	3.226	13	46	3.266	120,210
100	2.942	2.939	100	92	2.984	121,211
30	2.882	2.889	32	100	2.959	112
20	2.846	2.845	20	53	2.880	300
10	2.396	2.392	11	1	2.441	122,212
		2.224	1	6	2.267	302
5	2.372	2.368	6	1	2.396	130,310
35	2.139	2.141	16	15	2.199	113
		2.134	12	6	2.160	400
10	2.030	2.027	11	36	2.064	222
10	1.973	1.972	9	19	2.007	132,312
		1.958	4	9	1.982	230,320
25	1.918	1.914	27	26	1.960	123,213
25	1.890	1.888	24	22	1.914	231,321
5	1.861	1.863	7	23	1.885	140,410
20	1.833	1.831	20	29	1.862	402
5	1.782	1.783	7	12	1.838	004
		1.613	2	5	1.633	240,420
5	1.604	1.601	6	5	1.622	331
		1.560	4	9	1.602	124,214
		1.540	2	5	1.564	502
15	1.513	1.511	4	12	1.549	304
		1.511	9	8	1.541	233,323
10	1.500	1.499	11	10	1.518	151,511
		1.492	3	9	1.515	332
5	1.370	1.368	6	3	1.400	404
5	1.346	1.342	5	5	1.360	251,521
		1.321	2	7	1.341	602
				7	1.341	125,215
10	1.306	1.306	37	6	1.325	342,432
		1.304	7			125,215
10	1.289	1.288	3	14	1.316	144,414
		1.281	6	6	1.311	153,513

Note: The calculated pattern for pyromorphite is based on the structure data of Dai and Hughes (1989).

DISCUSSION

Phosphohedyphane has a $P6_3/m$ apatite structure (Fig. 2) with Ca and Pb ordered in the two nonequivalent large cation sites, with the Ca1(4*f*) site occupied mostly by Ca ($Ca_{0.92}Pb_{0.08}$) and the Ca2(6*h*) site occupied entirely by Pb. Similarly, Rouse et al. (1984) found virtually complete ordering in hedyphane: Ca1(4*f*): $Ca_{0.99}Pb_{0.01}$ and Ca2(6*h*): $Ca_{0.01}Pb_{0.99}$. The structure refinement of the synthetic hydroxyl analog of phosphohedyphane based on powder data by Engel et al. (1975) indicated essentially the same ordering scheme.

The apatite structure is well known for its ability to accommodate a wide variety of cations. Although the Ca1 and Ca2 sites can accommodate the same cations, they have quite distinct

TABLE 4. Data collection and structure refinement details for phosphohedyphane

Diffractometer	Bruker SMART Platform CCD
X-ray radiation/power	Mo*K*α (λ = 0.71073 Å)/50 kV, 45 mA
Temperature	298(2) K
Space group	$P6_3/m$
Unit-cell dimensions	a = 9.857(1) Å; c = 7.130(2) Å
Volume	599.9(2) Å^3
Z	2
Absorption coefficient	47.021 mm^{-1}
F(000)	924
Crystal size (**a** × **b** × **c**)	0.10 × 0.05 × 0.03 mm
Frame number/width/time	1271/0.3° in ω/30 s
θ range	2.39–28.23°
Index ranges	$-10 \le h \le 0$, $0 \le k \le 13$, $0 \le l \le 9$
Reflections collected	528
Independent reflections	528
Reflections, $F_o > 4\sigma(F_o)$	295
Completeness to θ = 28.26°	98.1%
Refinement method	Full-matrix least-squares on F^2
Parameters refined	41
GooF*	1.260
R indices [$F_o > 4\sigma(F_o)$]	$R(F)$† = 2.54%, w$R(F^2)$‡ = 4.52%
R indices (all data)	$R(F)$ = 3.06%, w$R(F^2)$ = 4.61%
Largest diff. peak/hole	+1.66/–1.19 *e*/Å^3

* GooF = $S = \{\Sigma[w(F_o^2 - F_c^2)^2]/(n-p)\}^{1/2}$.
† $R(F) = \Sigma||F_o| - |F_c||/\Sigma|F_o|$.
‡ $wR(F^2) = \{\Sigma[w(F_o^2 - F_c^2)^2]/\Sigma[w(F_o^2)^2]\}^{1/2}$; $w = 1/[\sigma^2(F_o^2) + (aP)^2 + bP]$ where a is 0, b is 12.994, and P is $[2F_c^2 + \text{Max}(F_o^2,0)]/3$.

TABLE 5. Atomic coordinates, occupancies and equivalent isotropic displacement parameters (Å^2) for phosphohedyphane

	x	*y*	*z*	occupancy	U_{eq}
Ca1	1/3	2/3	0.0068(3)	0.919(3)	0.014(1)
Pb1	1/3	2/3	0.0068(3)	0.081(3)	0.014(1)
Pb2	0.2574(1)	0.0083(1)	1/4	1	0.015(1)
P	0.4192(2)	0.3868(2)	1/4	0.907(8)	0.010(1)
As	0.4192(2)	0.3868(2)	1/4	0.093(8)	0.010(1)
O1	0.3677(8)	0.5099(8)	1/4	1	0.016(2)
O2	0.6029(8)	0.4681(8)	1/4	1	0.017(2)
O3	0.3640(7)	0.2801(6)	0.0761(8)	1	0.026(1)
Cl	0	0	0	1	0.017(1)

TABLE 6. Anisotropic displacement parameters (Å^2 × 10^3) for phosphohedyphane

	U_{11}	U_{22}	U_{33}	U_{23}	U_{13}	U_{12}
Ca1	0.014(1)	0.014(1)	0.015(1)	0	0	0.007(1)
Pb1	0.014(1)	0.014(1)	0.015(1)	0	0	0.007(1)
Pb2	0.010(1)	0.013(1)	0.020(1)	0	0	0.005(1)
P	0.008(1)	0.007(1)	0.014(1)	0	0	0.004(1)
As	0.008(1)	0.007(1)	0.014(1)	0	0	0.004(1)
O1	0.015(4)	0.012(4)	0.025(4)	0	0	0.010(3)
O2	0.005(3)	0.007(3)	0.038(5)	0	0	0.002(3)
O3	0.037(3)	0.025(3)	0.025(3)	–0.013(3)	–0.020(3)	0.022(3)
Cl	0.015(1)	0.015(1)	0.019(2)	0	0	0.008(1)

TABLE 7. Selected bond distances and angles in phosphohedyphane compared to those in hedyphane

	Phosphohedyphane	Hedyphane
Ca1-O1 (×3)	2.456(5) Å	2.38(2) Å
Ca1-O2 (×3)	2.519(5) Å	2.55(2) Å
Ca1-O3 (×3)	2.821(6) Å	2.86(2) Å
Pb2-O2	2.346(7) Å	2.36(3) Å
Pb2-O3 (×2)	2.547(6) Å	2.54(2) Å
Pb2-O3 (×2)	2.646(6) Å	2.67(2) Å
Pb2-Cl (×2)	3.0679(4) Å	3.117(2) Å
Pb2-O1	3.289(7) Å	3.45(2) Å
Pb2-O1	3.296(7) Å	3.45(2) Å
P/As-O1	1.531(7) Å	1.70(2) Å
P/As-O3 (×2)	1.539(6) Å	1.66(2) Å
P/As-O2	1.572(7) Å	1.73(3) Å
<P/As-O>	1.545 Å	1.69 Å
O1-P/As-O2	110.5(4)°	111(1)°
O1-P/As-O3 (×2)	113.4(3)°	115(1)°
O2-P/As-O3 (×2)	105.8(3)°	104(1)°
O3-P/As-O3	107.4(5)°	106(2)°

TABLE 8. Bond valence summations for phosphohedyphane

	O1	O2	O3	Cl	$\Sigma_c v$
$(Ca_{0.92}Pb_{0.08})$	$^{\times 2\downarrow}0.275^{\times 3\rightarrow}$	$^{\times 2\downarrow}0.232^{\times 3\rightarrow}$	$0.103^{\times 3\rightarrow}$		1.830
Pb	0.042	0.531	$0.309^{\times 2\rightarrow}$	$^{\times 6\downarrow}0.234^{\times 2\rightarrow}$	2.171
	0.041		$0.236^{\times 2\rightarrow}$		
$(P_{0.91}As_{0.09})$	1.267	1.134	$1.240^{\times 2\rightarrow}$		4.882
$\Sigma_a v$	1.900	2.130	1.888	1.402	

Notes: Bond strengths from Brese and O'Keeffe (1991); based upon refined occupancies shown. Valence summations are expressed in valence units.

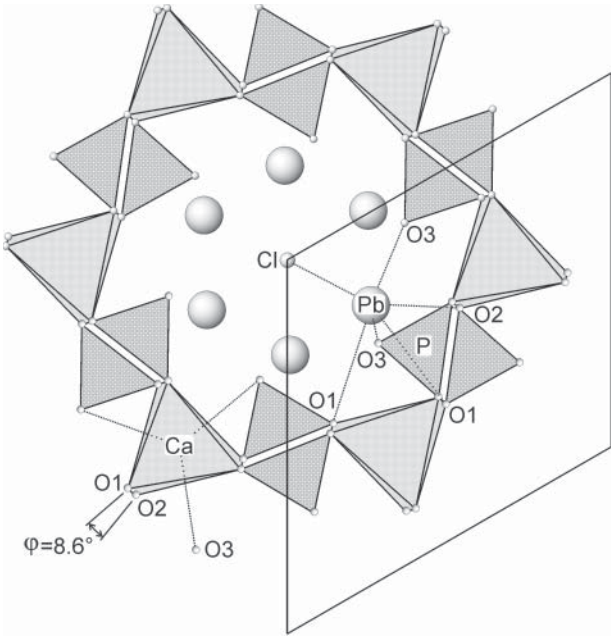

FIGURE 2. Phosphohedyphane crystal structure viewed down [001]. Pb-O,Cl and Ca-O3 bonds are shown.

coordinations. The Ca1 site is surrounded by three O1 and three O2 atoms in an arrangement that is a twisted trigonal prism, but which can be viewed as intermediate between a trigonal prism and an octahedron. In addition, three more distant equatorial O3 atoms yield a tri-capped trigonal prism. This polyhedron has also been named a "metaprism" (White and Dong 2003; Dong and White 2004a, 2004b; Mercier et al. 2005) and the amount of twisting, referred to as the metaprism twist angle (σ), is the angle O1-Ca1-O2 projected on (001) and theoretically ranges from 0 (trigonal prism) to 60° (octahedron). Actual metaprism twist angles in apatite structures vary from 5.2 to 26.7° (White and Dong 2003). The apatite structure can be regarded as a framework made up of tetrahedra and Ca1 metaprisms forming channels along *c* in which the Ca2 cations and halide or hydroxyl anions are located (White et al. 2005). (Note that this is a somewhat different than the traditional perspective, in which the channel is treated as only including the halide/hydroxyl anion sites.) Smaller twist angles yield larger Ca1 sites and larger diameter channels. Both phosphohedyphane and hedyphane have notably small metaprism twist angles, 8.6 and 5.2°, respectively. By comparison, the metaprisms in pyromorphite, mimetite, chlorapatite, and turneaureite have twist angles of 17.6, 21.1, 19.1, and 13.0° respectively.

The Ca2 site coordination in apatite structures is quite variable, being dependent on the cation in the site, the channel diameter, and the nature (and placement) of the channel anion (OH, F, Cl, etc.). In phosphohedyphane and hedyphane, Pb exhibits very similar "lop-sided" coordination (Fig. 3) with one very short bond to O2, four normal length bonds to O3, two normal length bonds to Cl and two very long bonds to O1 (see Table 7). Engel et al. (1975) attributed the preference of Pb^{2+} for the Ca2 site in $Ca_2Pb_3(PO_4)_3OH$ as being due to the ability of Pb^{2+} to form partially covalent bonds with O2. A more convincing explanation, offered by Rouse et al. (1984), argues that Pb^{2+} prefers the lop-sided coordination of the Ca2 site because it better accommodates the stereoactive $6s^2$ electron lone pair on the Pb^{2+}.

The role of the channel anion in apatite structures (often indicated as X) has been extensively studied (Hughes et al. 1989; Kim et al. 2000). This anion assumes positions at the center the channel at 0,0,z forming bonds to the peripheral cations in the Ca2 sites. The interaction between the channel anion and the cations in the Ca2 sites dictates the position of the anion. In fluorapatite, the relatively small F^- anion is situated on a mirror plane at 0,0,¼ at the center of a triangle formed by three Ca^{2+} cations. In chlorapatite, the larger size of the Cl^- anion "forces" it to assume a position displaced from the mirror plane. In most instances, the Cl^- anions are disordered in half-occupied sites above and below the mirror plane and the $P6_3/m$ space group is retained; however, in some cases the Cl^- anions are ordered resulting in a monoclinic structure ($P2_1/b$). In turneaureite, the arsenate analog of chlorapatite, the Cl^- anions are disordered over 0,0,z sites (Wardojo and Hwu 1996). In pyromorphite (Dai and Hughes 1989), mimetite (Calos and Kennard 1990), hedyphane and phosphohedyphane, the Cl^- anions are located at 0,0,0, midway between two triangles formed by Pb^{2+} cations in the Ca2 sites. Each Cl^- anion bonds to six Pb^{2+} cations in a nearly perfect octahedral configuration.

The consistent location of the Cl^- anion at 0,0,0 in the structures of pyromorphite, mimetite, hedyphane, and phosphohedyphane contributes to similar Pb^{2+} coordinations for their Ca2 sites. The Ca2 site is, in fact, remarkably similar among these structures, despite the variations in the cations

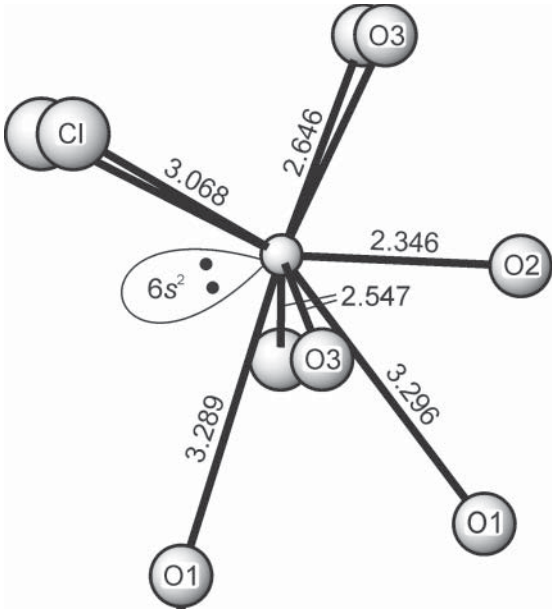

FIGURE 3. Representation of the Pb coordination in phosphohedyphane; the orientation is slightly canted with respect to the orientation in Figure 2. The likely approximate location of lone-pair electrons is shown.

occupying the Ca1 and tetrahedral sites in the framework. The metaprism twist, mentioned above, can be interpreted as a manifestation of the adjustment in the framework to effectively accommodate Pb^{2+} in the Ca2 site, thus explaining the small metaprism twist angles noted for phosphohedyphane and hedyphane.

The bond valence calculations for phosphohedyphane (Table 8) indicate reasonable valence sums for all cations and anions with the exception of Cl^-, which is significantly oversaturated (1.40 v.u.). The high bond valence sum for Cl^- results from relatively short Pb-Cl bonds (3.068), which are, in fact, significantly shorter than those in pyromorphite (3.111), mimetite (3.167), and hedyphane (3.117). There is no indication from either the chemical analyses or the structure refinement that the site at 0,0,0 is other than fully occupied by Cl alone. It might be inferred that the Pb-Cl bonds shorten and the Cl^- becomes more bond-oversaturated as the Ca^{2+} content in the Ca1 site increases, in response to the aforementioned adjustments in the framework to accommodate the Pb^{2+} coordination. Furthermore, it is clear that the structure is sufficiently stable to accommodate any local structural instability that may result from the Cl^- bond oversaturation.

CHEMICAL SOLID SOLUTION IMPLICATIONS

Chemical substitution and solid solution in compounds with the apatite structure, both natural and synthetic, have been extensively studied. A recent review has been provided by Pan and Fleet (2002). A complete solid solution has been shown to exist between pyromorphite, $Pb_5(PO_4)_3Cl$, and mimetite, $Pb_5(AsO_4)_3Cl$ (Kautz and Gubser 1969; Förtsch and Freiburg 1970) and the similarities between the structures of phosphohedyphane and hedyphane suggest that an analogous complete solid solution is likely to exist between them, as well.

Numerous synthetic studies have been conducted to determine the extent of solid solution between $Ca_5(PO_4)_3Cl$ (chlorapatite) and $Pb_5(PO_4)_3Cl$ (pyromorphite) and between $Ca_5(PO_4)_3OH$ (hydroxylapatite) and $Pb_5(PO_4)_3OH$ (Akhavan-Niaki 1961; Engel et al. 1975; Verbeeck et al. 1981; Miyake et al. 1986; Bigi et al. 1989). Although most of these have acknowledged the preference of Pb^{2+} for the Ca2 site, they have generally concluded there to be complete solid solutions in these series. However, more recent studies have brought into question the existence of complete solid solutions in the Ca-Pb apatite series. White et al. (2004) and Dong and White (2004a) demonstrated the existence of calcium and lead-rich nanodomains at unit-cell scales and showed that long annealing times of several weeks are necessary to completely equilibrate Ca-Pb partitioning in synthetic $(Pb_xCa_{10-x})(VO_4)_6F_2$. Dong and White (2004b) also provided evidence for a miscibility gap in this series.

In their description of hedyphane, $Ca_2Pb_3(AsO_4)_3Cl$, Rouse et al. (1984) suggested that the ordering of Ca^{2+} and Pb^{2+} could result in a solvus in the system $Ca_5(AsO_4)_3Cl$ (turneaureite)-$Pb_5(AsO_4)_3Cl$ (mimetite) and hence a miscibility gap. In support of this hypothesis, they provided analyses of minerals in this system from Franklin, New Jersey, and Långban, Sweden. Twelve of their analyses (which have the total of all non-Pb and Ca cations < 0.3) are plotted in Figure 4 along with the analyses from our EDS survey, the analyses in Table 2, and analyses of calcium-bearing "pyromorphite" and "mimetite" from Dana (1892) and Palache et al. (1951). Many compositions fall on or near the pyromorphite-mimetite, pyromorphite-phosphohedyphane and mimetite-hedyphane joins, suggesting that complete solid solutions exist for these series. Although intermediate compositions along the hedyphane-phosphohedyphane join were not noted, numerous intermediate analyses with somewhat lower Ca were found in the pyromorphite-phosphohedyphane-hedyphane-mimetite region. Just as Rouse et al. (1984) found essentially no intermediate compositions between hedyphane and turneaureite, our EDS survey showed none between phosphohedyphane and chlorapatite. These results, coupled with the lack of any reports of natural chlorapatite containing more than a trace of Pb, are strong evidence for a miscibility gap between phosphohedyphane and chlorapatite.

A mechanism to explain the existence of solid solution between and among pyromorphite, mimetite, hedyphane, and phosphohedyphane has already been alluded to. Continuous adjustments to the framework in the apatite structure via the twisting of the Ca1 metaprism allow a complete range of Pb^{2+} and Ca^{2+} substitution in the Ca1 site (and probably also P and As in the tetrahedral site), while maintaining a stable coordination for Pb^{2+} in the Ca2 site. A concentration of compositions between mimetite and phosphohedyphane seen in Figure 4 also suggests a possible relationship between Pb-Ca substitution in the Ca1 site and P-As substitution in the tetrahedral site. The apparent miscibility gap between hedyphane-phosphohedyphane and turneaureite-chlorapatite may be attributed to the coordination environment of the Ca2 site, which very strongly favors Pb^{2+} in hedyphane and phosphohedyphane (as well as in mimetite and pyromorphite) and which very strongly favors Ca^{2+} in chlorapatite and turneaureite. The structure presumably

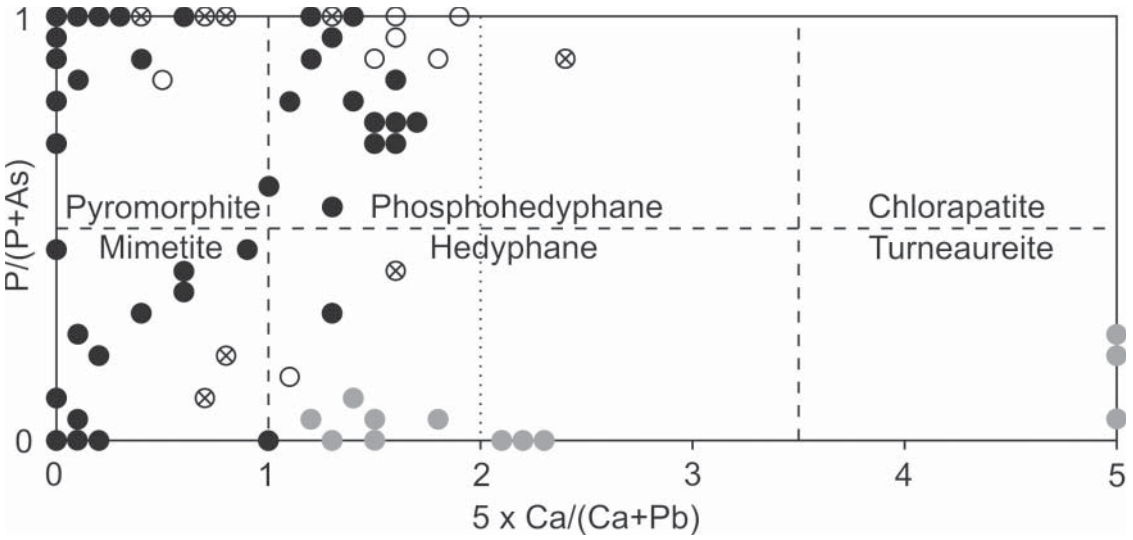

FIGURE 4. Distribution of compositions from the EDS survey (black circles), electron microprobe analyses in Table 2 (open circles), selected compositions (with non-Pb/Ca cations <0.3) of hedyphane and turneaureite from Rouse et al. (1984) (gray circles) and Ca-bearing "pyromorphite" and "mimetite" from Dana (1892) and Palache et al. (1951) (x-circles). P/(P + As) values are rounded to the nearest 0.05 and 5 × Ca/(Ca + Pb) values are rounded to the nearest 0.1. Some circles represent multiple points.

cannot adjust to create a stable Ca2 coordination environment for both Pb^{2+} and Ca^{2+}.

It is worthwhile to reiterate in this context the important role that the channel anion plays in the Ca2 site coordination. Although significant Pb content has not been reported in natural chlorapatite, Livingstone (1994) reported plumboan fluorapatite occurring as overgrowths on calcian phosphatian vanadinite from the Belton Grain vein, Wanlockhead, Scotland. Electron microprobe analyses showed the plumboan fluoroapatite to have Ca-Pb contents ranging from ($Ca_{4.65}Pb_{0.35}$) to ($Ca_{4.02}Pb_{0.98}$). This suggests that, with the smaller F^- as the channel anion, the Ca2 site is more tolerant of joint occupancy by Pb^{2+} and Ca^{2+}.

The much lower solubility of pyromorphite than apatite is the basis for recent research into the use of apatite to reclaim Pb-contaminated waters and soils. Pyromorphite has been shown to be a very stable and very low solubility environmental repository for lead under a wide variety of conditions (Chen et al. 1997). Manecki et al. (2000) showed that, under conditions approximating those in natural soils, fluorapatite, hydroxylapatite and chlorapatite react in aqueous solutions containing Pb^{2+} and Cl^- to form pyromorphite. Although the formation of compounds corresponding to calcian pyromorphite and/or phosphohedyphane were not reported in this study, some other soil studies have shown calcian pyromorphite to be a significant phase. Calcian pyromorphite has been identified as the major lead-bearing phase in mine waste soils from the South Pennine Orefield, England, (Cotter-Howells et al. 1994) and the Charterhaouse mine in the Mendip Hills, England, (Cotter-Howells and Caporn 1996). In experiments on the use of apatite amendments to Pb-contaminated soil (including associated grass roots) from a residential area near Oakland, California, Laperche et al. (1997) noted that, when the soils were treated with phosphate rock (containing fluorapatite as the major constituent), all pyromorphite formed contained significant Ca.

The apparent stability in natural systems of members of the chlorapatite-pyromorphite series between pyromorphite and phosphohedyphane, but not between phosphohedyphane and chlorapatite may have important implications for the use of apatite to reclaim Pb-contaminated waters and soils.

ACKNOWLEDGMENTS

Structure data collection was performed in the X-ray Crystallography Laboratory of the University of California, Los Angeles, Department of Chemistry and Biochemistry. Saeed Khan of that laboratory is acknowledged for technical assistance. Patrick Haynes provided several of the samples used in the EDS survey, including all of those from the Goodsprings district. N.V. Chunkanov and I.V. Pekov provided an electron microprobe analysis and background information on phosphohedyphane from Ken'-Choku, Kazakhstan. Maurizio Dini provided copies of the two unpublished reports on the Capitana mine. David I. Green provided the reference for plumboan fluorapatite from Wanlockhead, Scotland. John Rakovan, Maciej Manecki, Timothy J. White, and Cristiano Ferraris provided helpful comments on the manuscript. This study was funded by the John Jago Trelawney Endowment to the Mineral Sciences Department of the Natural History Museum of Los Angeles County.

REFERENCES CITED

Akhavan-Niaki, A.N. (1961) Contribution a l'étude des substitutions dans les apatites. Annales de Chimie, 6, 51–79.

Barruel (1836) Annales de Chimie et de Physique, Paris, 62, 217.

Bigi, A., Ripamonti, A., Brückner, S., Gazzano, M., Roveri, N., and Thomas, S.A. (1989) Structure refinements of lead substituted calcium hydroxyapatite by X-ray powder fitting. Acta Crystallographica, B45, 247–251.

Breithaupt, A. (1832) Vollständige Charakteristik des Mineral-System's, second edition. Dresden.

——— (1841) Vollständige Handbuch der Mineralogie, vol. 2, Dresden and Leipzig.

Brese, N.E. and O'Keeffe, M. (1991) Bond-valence parameters for solids. Acta Crystallographica, B47, 192–197.

Bruggen, J. (1938) Minas Capitana y porvenir ladrillos. Instituto de Investigaciones Geologicas, Santiago, Chile (unpublished report).

Bruker (1997) SADABS, SAINT, SMART and SHELXTL. Bruker AXS Inc., Madison, Wisconsin.

Calos, N.J. and Kennard, C.H.L. (1990) Crystal structure of mimetite, $Pb_5(AsO_4)_3Cl$. Zeitschrift für Kristallographie 191, 125–129.

Chen, X., Wright, J.V., Conca, J.L., and Peurrung, L.M. (1997) Evaluation of heavy metal remediation using mineral apatite. Water, Air, and Soil Pollution, 98, 57–78.

Chukhrov, F.V. (1952) Pyromorphite in steppe part of Kazakhstan. Trudy Mineralogicheskogo Muzeya, 4, 156–159. Proceedings of Mineralogical Museum, Academy of Science USSR, Moscow.

Cook, R.B. (1979) Chañarcillo, Chile. Mineralogical Record, 10, 197–204.

Cotter-Howells, J.D. and Caporn, S. (1996) Remediation of contaminated land by formation of heavy metal phosphates. Applied Geochemistry, 11, 335–342.

Cotter-Howells, J.D., Champness, P.E., Charnock, J.M., and Pattrick, R.A.D. (1994) Identification of pyromorphite in mine-waste contaminated soils by ATEM and EXAFS. European Journal of Soil Science, 45, 393–402.

Dai, Y.S. and Hughes, J.M. (1989) Crystal structure refinements of vanadinite and pyromorphite. Canadian Mineralogist, 27, 189–192.

Dana, E.S. (1892) System of Mineralogy, sixth edition. John Wiley and Sons, New York.

Dong, Z.L. and White, T.J. (2004a) Calcium-lead fluoro-vanadinite apatites: I. Disequilibrium structures. Acta Crystallographica, B60, 138–145.

——— (2004b) Calcium-lead fluoro-vanadinite apatites: II. Equilibrium structures. Acta Crystallographica, B60, 146–154.

Engel, G., Krieg, F., and Reif, G. (1975). Mischkristallbildung und kationenordnung im system bleihydroxylapatit-calciumhydroxylapatit. Journal of Solid State Chemistry, 15, 117–l 26.

Förtsch, E. and Freiburg, I.B. (1970) Untersuchungen as mineralien der pyromorphite gruppe. Neues Jahrbuch für Mineralogie Abhandlungen, 113, 219–250.

Hata, M., Marumo, F., Iwai, S., and Aoki, H. (1980) Structure of a lead apatite $Pb_9(PO_4)_6$. Acta Crystallographica, B36, 2128–2130.

Hughes, J.M., Cameron, M., and Crowley, K.D. (1989) Structural variations in natural F, OH, and Cl apatites. American Mineralogist, 74, 870–876.

Kautz, K. and Gubser, R. (1969) Untersuchungen mit der elektronen-mikrosonde an zonargebauten mineralien der pyromorphite gruppe. Contributions to Mineralogy and Petrology, 20, 298–305.

Kim, J.Y., Fenton, R.R., Hunter, B.A., and Kennedy, B.J. (2000) Powder diffraction studies of synthetic calcium and lead apatites. Australian Journal of Chemistry, 53, 679–686.

Laperche, V., Logan, T.J., Gaddam, P., and Traina, S.J. (1997) Effect of apatite amendments on plant uptake of lead from contaminated soil. Environmental Science and Technology, 31, 2745–2753.

Livingstone, A. (1994) Analyses of calcian phosphatian vanadinite, and apatite high in lead, from Wanlockhead, Scotland. Journal of the Russell Society, 5, 124–126.

Manecki, M., Maurice, P.A., and Traina, S.J. (2000) Kinetics of aqueous Pb reaction with apatites. Soil Science, 165, 920–933.

Mathew, M., Brown, W.E., Austin, M., and Negas, T. (1980) Lead alkali apatites without hexad anion: the crystal structure of $Pb_8K_2(PO_4)_6$. Journal of Solid State Chemistry, 35, 69–76.

Mercier, P.H.J., Le Page, Y., Whitfield, P.S., Mitchell, L.D., Davidson, I.J., and White, T.J. (2005) Geometrical parameterization of the crystal chemistry of $P6_3/m$ apatites: comparison with experimental data and ab initio results. Acta Crystallographica, B61, 635–655.

Miyake, M., Ishigaki, K., and Suzuki, T. (1986) Structure refinements of Pb^{2+} ion-exchanged apatites by X-ray powder pattern-fitting. Journal of Solid State Chemistry, 61, 230–235.

Palache, C., Berman, H, and Frondel, C. (1951) Dana's System of Mineralogy, seventh edition. Wiley, New York.

Pan, Y. and Fleet, M. (2002) Compositions of the apatite-group minerals: substitution mechanisms and controlling factors. In M.J. Kohn, J. Rakovan, and J.M. Hughes, Eds., Phosphates: Geochemical, Geobiological, and Materials Importance, vol. 48, p. 13–50. Reviews in Mineralogy and Geochemistry, Mineralogical Society of America, Chantilly, Virginia.

Raade, G. (2005) Ca-reicher und zonierter Pyromorphit vom Berg Aukas, Namibia. Mineralien Welt, 16, 58–59.

Risopatron, O. (1928) Informe sobre el reconocimiento de la Mina Capitana. Instituto de Investigaciones Geologicas, Santiago, Chile. (unpublished report).

Rouse, R.C., Dunn P.J., and Peacor, D.R. (1984) Hedyphane from Franklin, New Jersey and Långban, Sweden: cation ordering in an arsenate apatite. American Mineralogist, 69, 920–927.

Schneider, W. (1967) Caracolite, das $Na_3Pb_2(SO_4)_3Cl$ mit apatitstruktur. Neues Jahrbuch für Mineralogie Monatshefte, 284–298.

Segerstrom, K. (1960) Cuadrángulo Quebrada Paipote, Provincia de Atacama. Instituto de Investigaciones Geológicas, Carta Geológica de Chile, vol. 2, no 1.

Sheldrick, G.M. (1997) SHELXL97. Program for the refinement of crystal structures. University of Göttigen, Germany.

Verbeeck, R.M.H., Lassuyt, C.J., Helillgers, H.J.M., Driessens, F.C.M., and Vrollik, J.W.G.A. (1981) Lattice parameters and cation distributions of solid solutions of calcium and lead hydroxyapatites. Calcified Tissue International, 33, 243–247.

Wardojo, T.A. and Hwu, S.-J. (1996) Chlorapatite: $Ca_5(AsO_4)_3Cl$. Acta Crystallographica C52, 2959–2960.

White, T.J. and Dong, Z.L. (2003) Structural derivation and crystal chemistry of apatites. Acta Crystallographica, B59, 1–16.

White, T.J., Dong, Z.L., and Kim, J.Y. (2004) Nanoscale disequilibrium in waste form apatites. Transactions of the Materials Research Society of Japan, 29, 1977–1982.

White, T.J., Ferraris, C., Kim, J., and Srinivasan, M. (2005) Apatite—an adaptive framework structure. In G. Ferraris, and S. Merlino, Eds., Micro and mesoporous mineral phases. 57, 307–402. Reviews in Mineralogy and Geochemistry, Mineralogical Society of America, Chantilly, Virginia.

MANUSCRIPT RECEIVED MARCH 23, 2006
MANUSCRIPT ACCEPTED JUNE 8, 2006
MANUSCRIPT HANDLED BY SERGEY KRIVOVICHEV